Trehalose-6-Phosphate Synthase/Phosphatase Regulates Cell Shape and Plant Architecture in Arabidopsis[1][W][OA]

S. Narasimha Chary[2], Glenn R. Hicks, Yoon Gi Choi, David Carter, and Natasha V. Raikhel*

Center for Plant Cell Biology, Institute for Integrative Genome Biology (S.N.C., G.R.H., Y.G.C., D.C., N.V.R.), and Department of Botany and Plant Sciences (S.N.C., G.R.H., N.V.R.), University of California, Riverside, California 92521

The vacuole occupies most of the volume of plant cells; thus, the tonoplast marker δ-tonoplast intrinsic protein-green fluorescent protein delineates cell shape, for example, in epidermis. This permits rapid identification of mutants. Using this strategy, we identified the *cell shape phenotype-1* (*csp-1*) mutant in *Arabidopsis thaliana*. Beyond an absence of lobes in pavement cells, phenotypes included reduced trichome branching, altered leaf serration and stem branching, and increased stomatal density. This result from a point mutation in *AtTPS6* encoding a conserved amino-terminal domain, thought to catalyze trehalose-6-phosphate synthesis and a carboxy-terminal phosphatase domain, is catalyzing a two-step conversion to trehalose. Expression of *AtTPS6* in the *Saccharomyces cerevisiae* mutants *tps1* (encoding a synthase domain) and *tps2* (encoding synthase and phosphatase domains) indicates that AtTPS6 is an active trehalose synthase. *AtTPS6* fully complemented defects in *csp-1*. Mutations in class I genes (*AtTPS1–AtTPS4*) indicate a role in regulating starch storage, resistance to drought, and inflorescence architecture. Class II genes (*AtTPS5–AtTPS11*) encode multifunctional enzymes having synthase and phosphatase activity. We show that class II *AtTPS6* regulates plant architecture, shape of epidermal pavement cells, and branching of trichomes. Thus, beyond a role in development, we demonstrate that the class II gene *AtTPS6* is important for controlling cellular morphogenesis.

Cell shape is an important component of tissue and organ development and morphogenesis in all living organisms and shape is acquired during the process of cellular differentiation. In plants, most cells are immotile and attached to one another and, with few exceptions, are cylindrical. However, more complex shapes are found and include lobed pavement cells in the leaf epidermis of some species and trichomes of leaves and stems. Trichomes have been the subject of investigations into mechanisms that underlie cell shape determination in plants (Qiu et al., 2002; Deeks and Hussey, 2003; Smith, 2003; Wasteneys and Galway, 2003; Schellmann and Hulskamp, 2005). Mutants in maize (*Zea mays*) and Arabidopsis (*Arabidopsis thaliana*) have pointed toward the cytoskeleton as an important determinant of cell shape (Smith et al., 1996; Qiu et al., 2002; Mathur et al., 2003; Mathur, 2004) paralleling similar discoveries in animal cells. In lobed leaf pavement cells, transversely arranged bundles of microtubules (MTs) in neck regions alternate with regions of cortical fine actin microfilaments where there are no MTs to promote the outgrowth of lobes (Frank and Smith, 2002; Fu et al., 2002). By screening for mutants in pavement cell shape using a GFP marker to readily visualize morphology, we describe here an example of a completely new class of mutants that affect cell shape: mutants in trehalose-6-P synthases (TPSs)/trehalose-6-P phosphatases (TPPs).

Trehalose is a nonreducing disaccharide composed of two Glc units that is present in diverse organisms, such as bacteria, fungi, lichens, algae, and invertebrates (Augier, 1954; Elbein, 1974; Goddijn and van Dun, 1999; Elbein et al., 2003). Initially, trehalose was believed to be present only in desiccation-tolerant plants, such as *Selaginella lepidophylla* and *Myrothammnus flabellifolia* (Adams et al., 1990; Müller et al., 1995); however, more recently it has been demonstrated to be at low levels in all plants. Furthermore, a yeast (*Saccharomyces cerevisiae*) loss-of-function mutant in *trehalose-6-phosphate synthase1* (*tps1*) is complemented by the Arabidopsis homolog *AtTPS1*, indicating the presence of functionally equivalent biosynthetic genes in other plant species (Goddijn and Smeekens, 1998). In fact, all plants examined have the genes necessary for trehalose biosynthesis. Arabidopsis has 11 homologs encoding *TPS*s that are known to produce transcripts and are thus presumed to be functional. There is considerable evidence for a role of trehalose in protection from heat, osmotic, nutrient, and dehydration stress, as well as toxic chemicals. It may also play a protective role in the oxidative stress of proteins and lipids (Wiemken, 1990; Crowe et al., 1992; Newman et al., 1993; Fillinger et al.,

[1] This work was supported by the Department of Energy (grant no. DE–FG03–02ER15295/A000 to N.V.R.).

[2] Present address: Dow AgroSciences LLC, 9330 Zionsville Rd., Indianapolis, IN 46268.

* Corresponding author; e-mail nraikhel@ucr.edu.

The author responsible for distribution of materials integral to the findings presented in this article in accordance with the policy described in the Instructions for Authors (www.plantphysiol.org) is: Natasha V. Raikhel (nraikhel@ucr.edu).

[W] The online version of this article contains Web-only data.

[OA] Open Access articles can be viewed online without a subscription.

www.plantphysiol.org/cgi/doi/10.1104/pp.107.107441

2001) and has been shown to function in carbohydrate storage (Elbien et al., 2003).

Beyond these more established roles of *TPS* genes in plants, recent intriguing evidence has implicated these genes as important modulators of plant development and inflorescence architecture. In one dramatic example, trehalose appears to modulate inflorescence branching in maize (Satoh-Nagasawa et al., 2006). Inflorescence branching in maize is controlled by the *RAMOSA* genes, and one of the genes (*RAMOSA3*) encodes a trehalose biosynthetic gene that functions through the regulation of the transcription factor RAMOSA1 (Satoh-Nagasawa et al., 2006). The results indicate that inflorescence architecture is controlled either by trehalose or, even more exciting, by a more direct transcriptional mechanism involving the protein. Other impacts on development by *TPS* genes have also been reported (see below).

The most common biosynthetic pathway for trehalose in plants is transfer of Glc from UDP-Glc to Glc-6-P resulting in trehalose-6-P and UDP. This initial step is catalyzed by TPS. In a second step, the dephosphorylation of trehalose-6-P occurs via TPP producing trehalose. In yeast, a large enzyme complex displaying both TPS and TPP catalytic activity is well described, and the *ScTPS1* gene and trehalose have been shown to be involved in stress protection and control of sugar flux into the glycolytic pathway via inhibition of hexokinase II (Bonini et al., 2000; van Vaeck et al., 2001). A *TPS1* yeast deletion mutant does not grow on Glc as a carbon source (Van et al., 1993), suggesting that trehalose can act as a signaling molecule. Among Arabidopsis homologs, only *AtTPS1* is well characterized (Blázquez et al., 1998; Gómez et al., 2006). It is a class I *TPS* gene in that it possesses an N-terminal synthase domain but lacks the C-terminal phosphatase domain (Leyman et al., 2001). Expression of *AtTPS1* has been linked to carbon metabolism and specific developmental phenotypes, such as delayed embryo development, altered root and shoot growth, and altered transition to flowering (Blázquez et al., 1998; van Dijken et al., 2004). Homozygous null mutants of *AtTPS1* are embryo lethal, displaying cell wall thickening and altered morphology (Gómez et al., 2005, 2006). There is also evidence for a role in stress tolerance (Romero et al., 1997; Pilon-Smits et al., 1998).

In tobacco (*Nicotiana tabacum*), expression of *Escherichia coli TPS* (*OTS A*) results in increased photosynthetic activity, stunted growth, and lancet-shaped leaf morphology, whereas constitutive expression of *TPP* (*OTS B*) results in reduced photosynthesis (Paul et al., 2001; Pellny et al., 2004). Pleiotropic effects in growth and development have also been observed in Arabidopsis as a result of *OTS A* and *OTS B* expression (Schluepmann et al., 2003). The effects are not due to increased trehalose accumulation, but rather to an increase of the intermediate trehalose-6-P, which may act as an important signaling molecule (Jang et al., 2003; Schluepmann et al., 2003). More recently, expression of genes encoding *TPS1* and *TPS2* of yeast were found to affect root growth in Arabidopsis as well impart drought tolerance (Karim et al., 2008).

Here, we describe the identification and analysis of a *cell shape phenotype-1* (*csp-1*) mutant that has a dramatic cellular effect in the leaf epidermis, resulting in loss of pavement cell lobes. In addition, *csp-1* impacts the cell morphology of trichomes, resulting in an altered pattern of branching. The mutant shows a range of developmental defects that include reduced stature, altered stem branching, and pronounced leaf serrations. A mutation was found in the *AtTPS6* gene. Significantly, we provide evidence indicating that this class II *TPS* gene functions in the control of cell morphology in addition to functioning as a broad modifier of whole-plant developmental phenotypes.

RESULTS

The *csp-1* Mutant Displays Multiple Cellular and Developmental Phenotypes in Arabidopsis

Previously, we reported a microscopy-based screen to identify vacuole-defective mutants (Avila et al., 2003) using tonoplast marker GFP fused to δ-tonoplast intrinsic protein (35S:GFP::δ-TIP; Cutler et al., 2000). Laser-scanning confocal microscopy analysis of the cellular phenotype showed that the leaf pavement cells of the parental Arabidopsis line expressing GFP::δ-TIP were typical in having pronounced lobes resulting in a jigsaw puzzle-like appearance, whereas pavement cells of *csp-1* showed either no lobes or lobes that were much less pronounced (Fig. 1, A and B). In addition to the loss of pavement cell lobes, the mutant displayed retarded development (see Fig. 2A), which in part may have accounted for a decrease in the size of individual cells in the hypocotyls compared to the parental line (Fig. 1, C and D). Root cells also appeared to be reduced in size (Fig. 1, E and F). Scanning electron micrographs of leaves of the *csp-1* mutant and the parental line also clearly highlighted the altered pavement cell shape (Fig. 1, G and H). Interestingly, the surface morphology of the mutant cells was more deeply ridged in appearance compared to the parental line. A trichome branching phenotype was obvious in the mutant (Fig. 1, I–K). In the mutant, 98% of trichomes (n = 10 seedlings; four to six leaves per seedling for a total of 842 trichomes) displayed two branches compared to the parental line in which 100% of trichomes had three branches (n = six seedlings; one to three leaves per seedling for a total of 191 trichomes). Quantification of individual trichome branches of *csp-1* indicated that, although the mutant produced fewer branches, they were longer than those of the parental line (Table I). The mutant displayed more stomates per unit area in *csp-1* (mean of 295/mm^2; n = 5 seedlings; three to four leaves per seedling) compared to the parental line (mean of 227/mm^2; n = 5 seedlings; three to four leaves per seedling), indicating an impact on mechanisms controlling stomatal density.

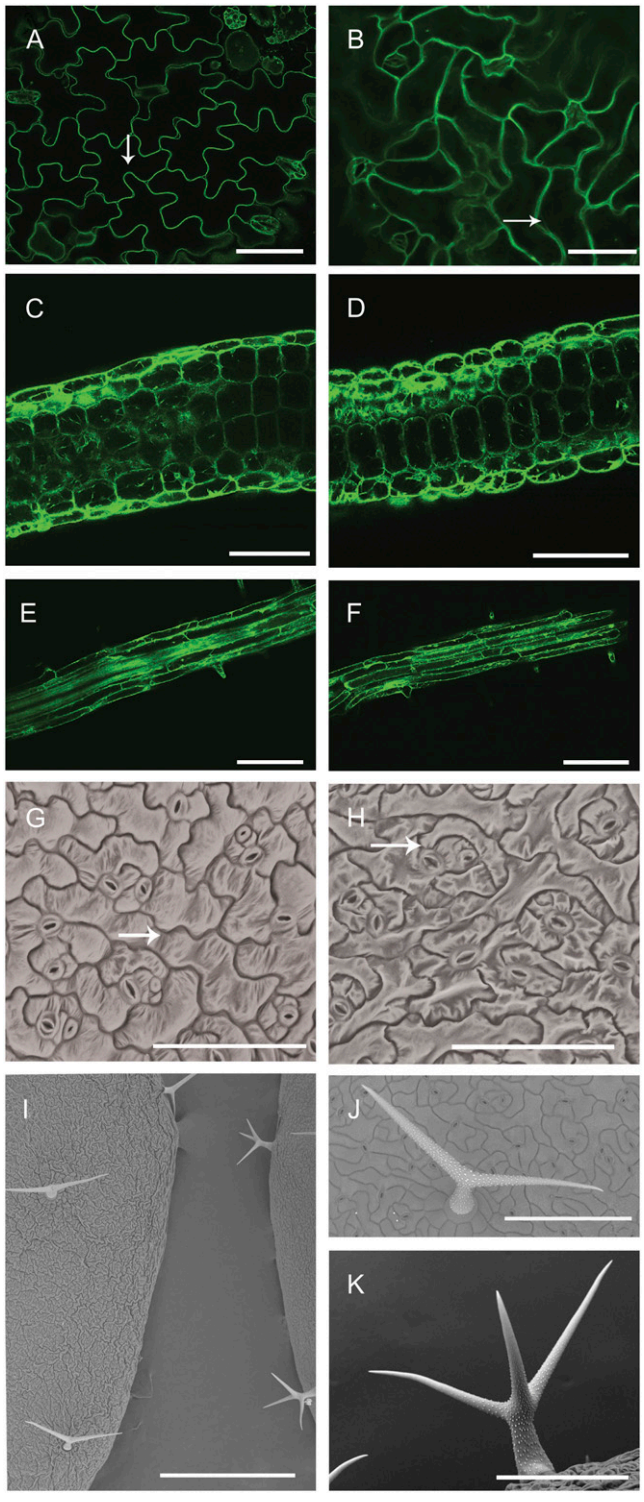

Figure 1. The *csp-1* mutant displays cell shape, size, and trichome aberrations. A to F, Confocal microscopy images of cells of 7-d-old seedlings expressing the tonoplast marker GFP::δ-TIP. A and B, Leaf epidermal pavement cells of parental (A) and *csp-1* mutant lines (B). C and D, Hypocotyl cells of the parent (C) and mutant (D). E and F, Root cells of the parent (E) and mutant (F). G to K, Scanning electron microscopy images of similar 14-d-old seedlings. G and H, Leaf epidermal pavement cells of the parental line (G) and mutant (H). I, Leaves of the *csp-1* mutant (left) and the parental line (right) display obvious differences in trichome biogenesis. J and K, Several individual trichomes are shown from *csp-1* (J) and the parental line (K), highlighting the differences in branch number. Arrows indicate positions of several epidermal cell lobes in the parent (A and G) and mutant (B and H). Bars = 50 μm (A and B); 150 μm (C–F); 100 μm (G and H); 500 μm (I); and 200 μm (J and K).

Beyond changes in cellular morphology and stomatal density, the mutant displayed retarded development. The stature and morphology of both 10-d-old seedlings (Fig. 2A) and adult plants (Fig. 2, B and C) of *csp-1* were significantly different from the parental line. The mutant exhibited slow growth at the seedling stage and rosette leaves of the mutant were greatly reduced in size and narrower than the parental line, with pronounced serration (Fig. 2D). Mutant leaves displayed strong epinasty (downward folding; Fig. 2, C and D). At bolting, the mutant showed a greater number of primary shoots than the parental line, each of which displayed reduced branching and delayed flowering, suggesting a reduction in apical dominance (data not shown).

Mapping of the *csp-1* Locus via Microarrays

To understand the basis of the cellular and developmental phenotypes associated with *csp-1*, we initiated a map-based cloning strategy to identify the locus and clone the mutated gene. The mutant in ecotype Columbia (Col) was crossed to Landsberg *erecta* (L*er*) to obtain segregating populations for mapping. Individuals from the F2 mapping population were scored for the mutant *csp* via confocal microscopy. We utilized a high-throughput screening method for scoring and screened more than 5,000 recombinants (see ''Materials and Methods''). In our (see ''Materials and Methods''). In our mapping population, *csp-1* displayed segregation that was consistent with a recessive mutation (data not shown). To map the mutation, the ATH1 Arabidopsis expression array was used (Borevitz et al., 2003). The array contained 22,500 probe sets representing 24,000 genes. Based on hybridization to a pool of 100 F2 recombinants and differences in allelic frequencies (Borevitz et al., 2003), we predicted that *csp-1* resided on the lower arm of chromosome 1 between 9.11 and 12.09 Mb with the maximal frequency at 10.60 Mb (Supplemental Fig. S1). We observed a minor statistical peak on chromosome 4 between 8.14 and 9.8 Mb; however, we confirmed the position of the *csp-1* locus on chromosome 1 between the insertion-deletion markers nga280 (83.83 cM) and nga111 (115.55 cM). The position was also confirmed using simple sequence length polymorphism markers on chromosome 1 (Bell and Ecker, 1994; data not shown). The locus was located on bacterial artificial chromosome (BAC) T23K23, which was 101.966 kb in length and contained 38 genes (Fig. 3A). Sequence analyses of all 38 genes revealed a single mis-sense

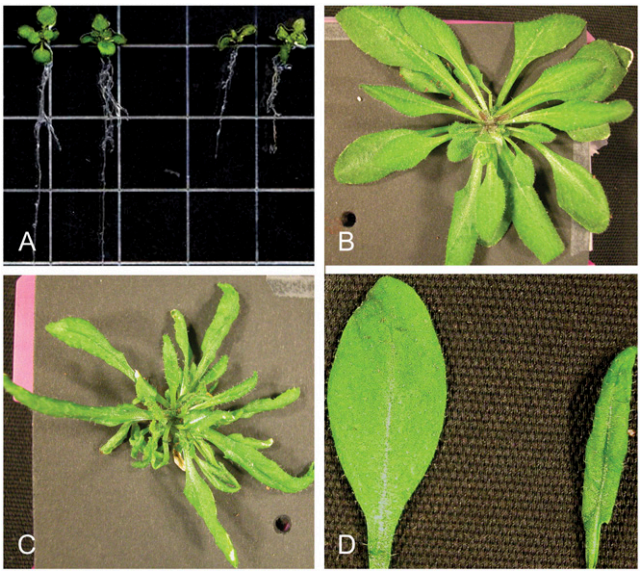

Figure 2. The *csp-1* mutant is affected in growth from seedling to adult stages. A, Nine-day-old seedlings of the parental line (left two seedlings) and *csp-1* (right two seedlings) show obvious retardation in growth of the mutant when grown and viewed on agar medium. B and C, Sixteen weeks after sowing, rosettes of the parent (B) and mutant (C) are different morphologically, with the leaves of *csp-1* displaying prominent serration and strong epinasty. D, Differences in leaf morphology are apparent when leaves of the parent (left leaf) are viewed in more detail relative to a mutant leaf (right leaf).

mutation at codon 160 of gene At1G68020.1. The gene was annotated in the Arabidopsis genome database as a glycosyl transferase family 20 protein/trehalose-phosphatase family protein similar to TPS of yeast. A substitution at nucleotide position 456 (A to C change) resulted in an Arg-to-Ser substitution in the protein (Fig. 3, B and C). Comparative analysis revealed that this Arg is a unique residue in TPS6 among class II TPS proteins (Supplemental Fig. S2).

csp-1 Is a Class II TPS Family Member

The mutated gene in *csp-1* encodes *TPS6* (*AtTPS6*). It has an open reading frame of 2,103 nucleotides encoding a polypeptide of 701 amino acids. The full-length genomic region of 3,081 nucleotides encodes one exon and no introns. In the Arabidopsis genome, there are 11 *AtTPS* genes that are grouped into two classes based on the homology to the TPS proteins of yeast. Class I consists of four genes containing amino-terminal synthase domains and class II consists of seven genes possessing both amino-terminal synthase and carboxyl-terminal phosphatase domains. The AtTPS6 protein contains both domains and is thus a class II TPS most similar to yeast TPS2 (Fig. 4A) and encodes both enzymatic activities necessary for trehalose biosynthesis. By comparison, AtTPS1 is a class I TPS (Leyman et al., 2001). Based on comparisons of the amino-terminal synthase and carboxyl-terminal phosphatase regions, class I and class II Arabidopsis TPS proteins fall into two distinct clades (Supplemental Fig. S3A). Gene expression of *AtTPS6* was in all organs examined in Arabidopsis, including seedling, rosette leaf, cauline leaf, flower, root, and silique (Supplemental Fig. S3B). We also analyzed *AtTPS6* mRNA accumulation in *csp-1* and the transcript was detected in the mutant (Supplemental Fig. S3C), suggesting that the mutation altered protein function but did not alter gross gene expression.

AtTPS6 Plays an Important Role in Cell Shape and Encodes Functional Domains Involved in Trehalose Biosynthesis

Yeast *TPS1* encodes a TPS, whereas *TPS2* encodes a TPP. A *tps1* mutant cannot grow on Glc as a carbon source because trehalose is necessary for the regulation of glycolysis by negatively regulating hexokinase II in vivo (Blázquez et al., 1993). A *tps2* deletion mutant in yeast showed reduced trehalose accumulation and an accompanying increase in thermosensitivity (De Virgilio et al., 1993). Because AtTPS6 possessed both synthase and phosphatase domains, we hypothesized that it would complement both *tps1* and *tps2* deletion mutant phenotypes in yeast if fully functional. Indeed, *AtTPS6* complemented the Glc sensitivity of the synthase-deficient mutant *tps1* and thermosensitivity of the phosphatase-deficient mutant *tps2* of yeast (Fig. 4B). These results indicate that *AtTPS6* is a multifunctional enzyme encoding functional synthase and phosphatase domains.

The complete *AtTPS6* coding region plus 5′ and 3′ regulatory regions (*TPS6Pro*::*TPS6*) was amplified using gene-specific primers from genomic DNA and cloned into a modified pBIN19-GW binary vector. The construct was used to transform *csp-1* mutant plants for complementation (Clough and Bent, 1998). Several transgenic lines were isolated that were kanamycin resistant and displayed complete restoration of pavement cell morphology (Fig. 5A) when compared to *csp-1* (Fig. 1B) and similar to the parental line (Fig. 1A).

Also restored were normal leaf shape, growth (Fig. 5, B and C), and typical trichomes with three branches (Fig. 5D). These results indicate that *AtTPS6* complemented the cell shape defects (pavement cells, trichomes) and overall growth phenotypes displayed by the *csp-1* mutant. We concluded that *AtTPS6* plays a significant role in modulating cellular shape as well as growth and development in Arabidopsis.

Table I. *Trichome branch length (μm)*

All measurements ± SE; $n = 15$ trichomes for each measurement. For *csp-1*, branch 3 not observed. Parental line is Col-0 expressing GFP::δ-TIP.

	Branch 1	Branch 2	Branch 3
Parental	191.7 ± 11.7	154.5 ± 6.6	143.2 ± 11.2
csp-1	231.8 ± 13.6	223.5 ± 12.2	None

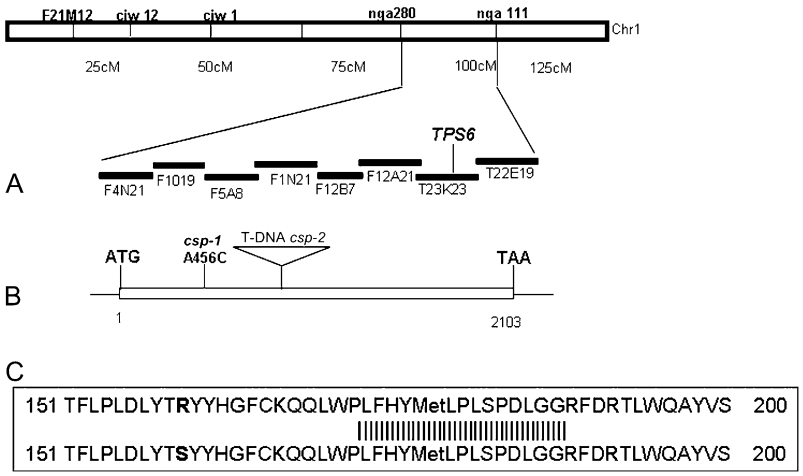

Figure 3. The *csp-1* mutant is altered in a gene encoding TPS (*AtTPS6*). A, The physical position of the *csp-1* locus is indicated with the positions of nearby insertion-deletion markers (top bar). The location of *AtTPS6* on BAC T23K23 is indicated with other BACs in the region. B, Schematic of the *AtTPS6* gene indicating start and stop codons. The positions of an A-to-C substitution in *csp-1* at nucleotide position 456 and a T-DNA allele (*csp-2*) are shown. Numbers indicate nucleotide positions. C, Amino acid residues in single-letter code are shown for the parental line (top sequence) and *csp-1* (bottom sequence) in the region of an Arg-to-Ser substitution (indicated by line). Numbers indicate amino acid positions.

Disruption and Overexpression of *AtTPS6* Dramatically Altered Cell and Developmental Phenotypes

A T-DNA insertion mutant (Alonso et al., 2003) from the SALK collection (*csp-2*) was characterized at the molecular and phenotypic levels. Genotyping of *csp-2* using the left border primer LbB1 and a gene-specific reverse primer indicated the position of the insertion in *AtTPS6* (Fig. 3B). The T-DNA insertion was in the exon at position 9 nucleotides within the synthase domain and abolished *AtTPS6* mRNA accumulation as evidenced by semiquantitative RT-PCR analysis (data not shown). Pavement cells were stained with FM4-64. This dye, which stains the plasma membrane, endomembranes, and vacuole, will also bind to the cell wall conveniently outlining cell shape. This staining revealed a cell shape defect in *csp*-2 similar to that observed in *csp-1* (Fig. 6A; compare to Fig. 1B). Interestingly, the *csp*-2 loss-of-function mutant did not display other developmental leaf phenotypes, such as pronounced serration, epinasty, and reduced trichome branching, as observed in *csp-1* (Fig. 6B; compare to Fig. 2C). This indicated that control of cell shape was separable genetically from developmental defects such as leaf morphology and expression of the mutated gene (*csp-1*) and complete loss of function (*csp-2*) resulted in cell shape defects. Loss-of-function mutants in the remaining class II *AtTPS* genes *AtTPS5*, *AtTPS7*, *AtTPS8*, *AtTPS9*, *AtTPS10*, and *AtTPS11* were also stained with FM4-64 and revealed no cell shape defects as observed in the *AtTPS6* mutants *csp-1* and *csp*-2 (data not shown). These results indicate that *AtTPS6* is unique among class II *AtTPS* genes in affecting the cell shape of leaf pavement cells.

To further investigate the role of *AtTPS6* in development, the coding region of *AtTPS6* was overexpressed in Arabidopsis under the control of the constitutive 35S promoter. The overexpression lines displayed an increase in *AtTPS6* transcript as detected by multiplex semiquantitative RT-PCR (data not shown). The phenotypes displayed by eight independent lines overexpressing *AtTPS6* were striking and related to those displayed by *csp-1*. For example, at 3 weeks old, the rosette leaves and overall stature of the plants were significantly greater than those of the parental line (Figs. 6C and 2B, respectively). In addition to these developmental phenotypes, the trichomes of all overexpression lines displayed an increased number of trichome branches, ranging from four to six compared to the parent, which displayed three branches (Figs. 6D and 1K, respectively).

The independent lines displayed a range of related phenotypes correlated with their levels of *AtTPS6* expression. We classified these lines into two general categories. For lines in category 1, the greatest amount of transcript was detected (Fig. 6E, inset), as well as a dramatic increase in the overall size and number of rosette leaves (Fig. 6E) and fewer bolts, suggesting an increase in apical dominance. Among category 2 overexpression lines, there was a more modest increase in expression (Fig. 6F, inset), resulting in fewer leaves, each having reduced serration compared to category 1 mutants. Overall growth was also slower than that of the category 1 lines (Fig. 6F). There was an apparent reduction in apical dominance as evidenced by increased primary shoots emerging from the rosette. There was also an increased number of flowering branches with altered leaf phyllotaxy compared to the parental line (data not shown). Overall, these results indicate that *AtTPS6* plays a role not only in establishing cellular morphology, but also in the overall growth and morphology of the organism.

DISCUSSION

We have shown that the *CSP* gene plays a critical role in the regulation of cell morphogenesis and other developmental processes. Interestingly, *CSP* encodes the multifunctional enzyme AtTPS6, suggesting that sugars are capable of regulating cell morphogenesis in plants, a process that is dependent upon signal-mediated

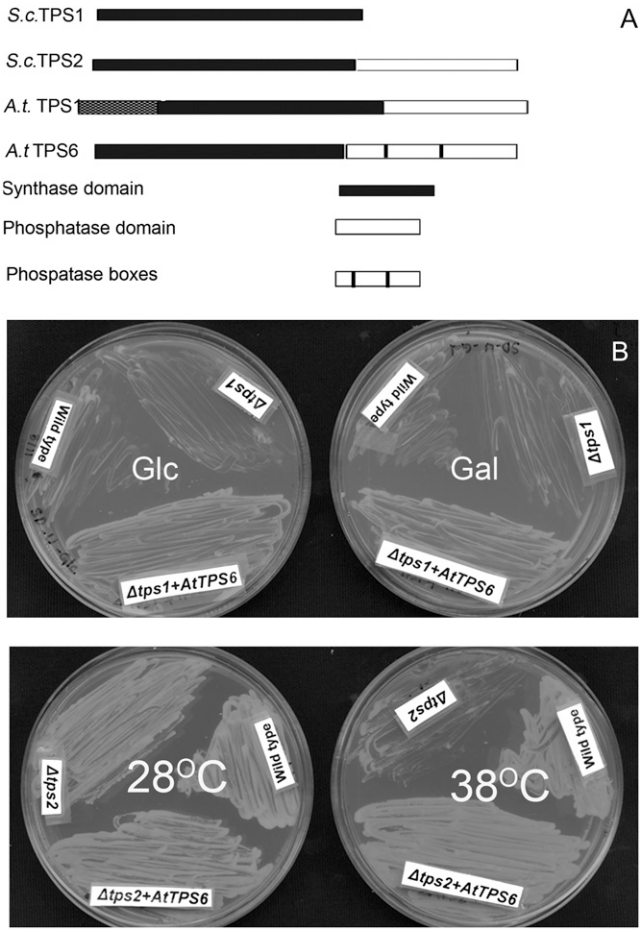

Figure 4. AtTPS6 has functional synthase and phosphatase domains. A, Schematic showing protein domains of TPS1 and TPS2 from yeast ScTPS1 and ScTPS2 and their homologs in Arabidopsis AtTPS1 and AtTPS6, respectively. B, Complementation of yeast with corresponding Arabidopsis genes. Top, As a control, wild-type yeast (wild type), a *ScTPS1* deletion mutant (*Δtps1*), and the deletion mutant expressing *AtTSP6* (*Δtps1* + *AtTPS6*) grew on Gal as a carbon source. When grown on Glc, wild-type yeast grew normally, whereas the deletion mutant (*Δtsp1*) could not utilize Glc as a carbon source. When *AtTPS6* was expressed in *Δtps1* (*AtTPS6* + *Δtps1*), yeast grew vigorously, indicating that *AtTPS6* complemented *Δtsp1* functionally. Bottom, When grown at the permissive temperature (28°C), wild-type yeast, a deletion mutant (*Δtps2*), and *AtTPS6* expressed in *Δtps2* (*Δtps2* + *AtTPS6*) all grew normally. However, at the nonpermissive temperature, *Δtps2* could not grow, whereas the strain expressing *AtTPS6* (*Δtps2* + *AtTPS6*) displayed growth similar to that of the control (wild type), indicating functional complementation by *AtTSP6*.

cytoskeletal dynamics and reorganization (Smith and Oppenheimer, 2005). Although the cytoskeleton has been shown to influence plant sensitivity to sugar responses, our results demonstrate that a class II TPS/TPP enzyme involved in sugar catabolism has a role in the control of cell morphogenesis. We have also found that *CSP* modulates a multitude of other developmental processes, such as plant stature, leaf morphology, shoot apical dominance, and root development. Overall, our findings support a concept in which AtTPS6 is an important regulator of plant development via a role in generating a sugar-based signal or more directly by participating in transcriptional regulation.

AtTPS6 Is Functionally Equivalent to TPS and TPP of Yeast

The TPS proteins from organisms as distant as bacteria, yeast, and plants are highly conserved at both the structural and functional levels; these similarities suggest evolutionarily conserved functions. Among the 11 Arabidopsis *TPS* genes, only *AtTPS1*, a class I gene possessing the synthase domain alone, has been investigated functionally (Leyman et al., 2001). Previous studies indicated that AtTPS7 and AtTPS8 may be inactive enzymatically in Arabidopsis (Vogel et al., 2001). Thus, we asked whether AtTPS6 was active functionally. Our data show that the gene is expressed in all organs examined in Arabidopsis, arguing that the gene is functional and ubiquitous. Furthermore, because *AtTPS6* possesses both synthase and phosphatase domains, we predicted that the gene would complement yeast deletion mutants of both *tps1* (synthase domain only) and *tps2* (phosphatase domain only). Validation of this prediction strongly indicates that AtTPS6 is an active class II bifunctional enzyme.

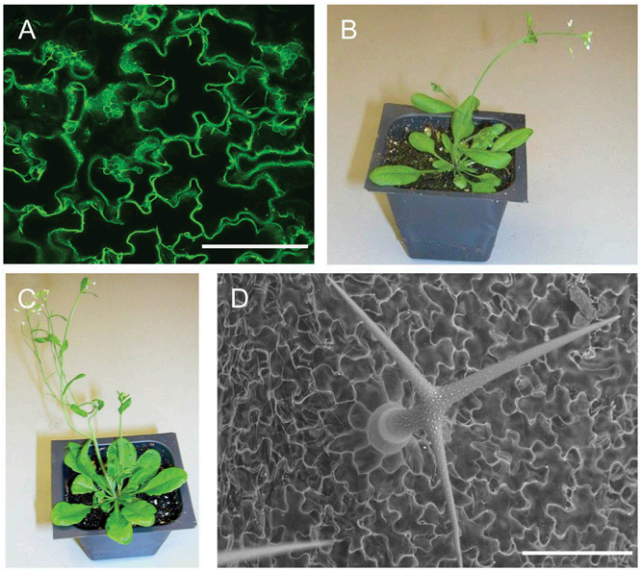

Figure 5. *AtTPS6* fully complements the cell shape and developmental defects in *csp-1*. A, Cell morphology of leaf pavement cells of 7-d-old Arabidopsis seedlings coexpressing GPF::δ-TIP and a construct encoding wild-type *AtTPS6* (*TPS6Pro*::*TPS6*; compare to Fig. 1, A and B). Normal cell morphology indicated complementation. B and C, Adult plants of the complemented mutant (C) displayed overall morphology similar to that of the control (wild type; B), including rosettes with leaves showing typical morphology without pronounced serration as in *csp-1* (compare to Fig. 2C). D, Trichome of the complemented line displaying three branches.

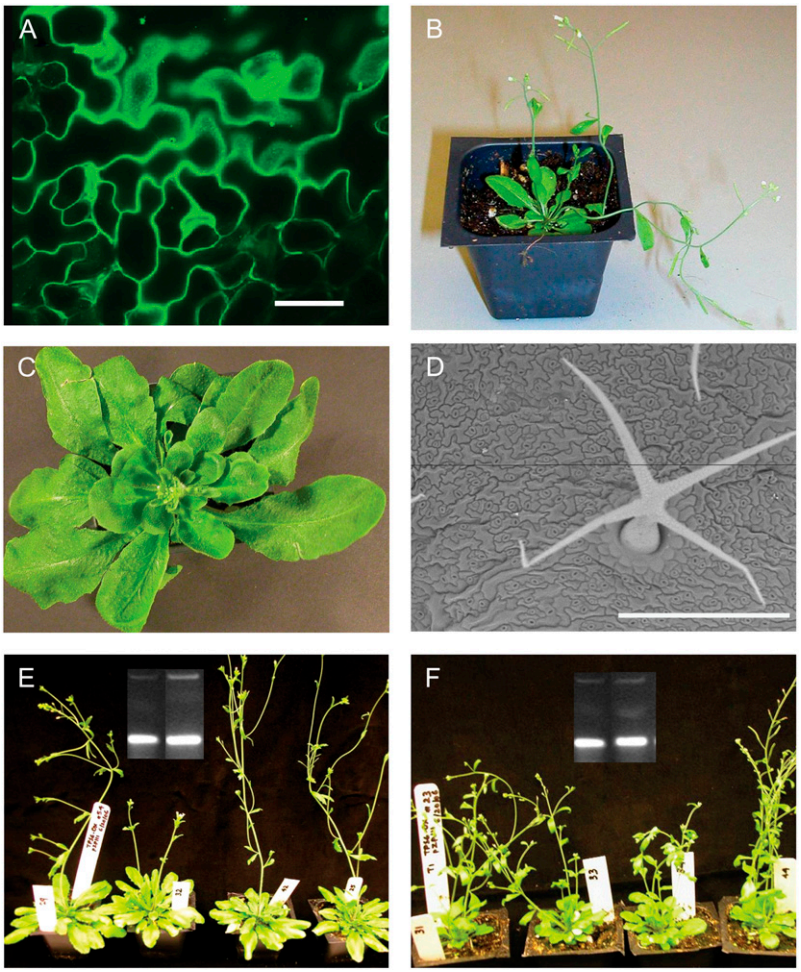

Figure 6. A second allele (*csp-2*) displays cell shape defects and overexpression lines of AtTPS6 showing dramatic alterations in development. A, A T-DNA loss-of-function allele *csp-2* when stained with FM4-64 also shows cell shape defects similar to those of *csp-1*. Bar = 50 μm. B, However, *csp-2* does not display leaf serration or epinasty as observed for *csp-1*. C, Representative category I overexpression mutant displaying increased rosette and leaf size. D, Scanning electron micrograph showing a representative trichome from a line overexpressing *AtTPS6* with four branches compared to the normal three found in the parental line (compare to Fig. 1K). Bar = 300 μm. E, Category I *AtTPS6* overexpression lines displaying increased rosette and leaf size and decreased bolts (increased apical dominance). Inset, Representative quantity of transcript by RT-PCR (top band, AtTPS6; bottom band, ribosomal control; left lane, wild-type Col ecotype; right lane, representative overexpression line). F, Category II *AtTPS6* overexpression lines displaying delayed growth and increased bolts (reduced apical dominance) but not enlarged rosettes. Inset, Representative quantity of transcript by RT-PCR (top band, AtTPS6; bottom band, ribosomal control; left lane, wild-type Columbia ecotype; right lane, category II overexpression line).

TPS6 Is a Class II Enzyme That Controls Cellular Morphology and Modifies Growth and Development

We found that the mutation in *csp-1* conferred pavement and trichome cell shape defects in addition to several strong developmental phenotypes, including altered leaf size and morphology, reduced plant stature, and increased stem branching. These phenotypes indicate that *AtTPS6* plays an important role not only in controlling cellular morphogenesis, but also in modifying overall development. Interestingly, it was reported that the Arabidopsis class I *tps1* mutant displays defects including embryo lethality and an effect on the transition to flowering (van Dijken et al., 2004). However, these phenotypes are different from those of *csp-1*. In any event, there are no reports to date describing developmental defects associated with class II TPS members, much less dramatic alterations in cell shape.

Among the cellular morphology phenotypes in *csp-1*, we observed two-branched trichomes. In Arabidopsis, there are at least 24 genes known to regulate trichome morphogenesis and branching (Oppenheimer, 1998) and there may be several redundant pathways. One of the branching mutants is regulated by the transcription factor basic helix-loop-helix that affects endoreduplication (Oppenheimer, 1998). However, there is also an endoreduplication independent pathway in trichome branch patterning. This work describes the involvement of *TPS* genes in trichome development. Complementation studies of the point mutant line *csp-1* demonstrated the restoration of all cellular and developmental defects, indicating that the synthase domain where the mutation resides is critical for modifying development and cellular morphology, including that of trichomes. This is further substantiated by the finding that overexpression of *AtTPS6* in Arabidopsis results in increased trichome branching as well as the restoration of typical pavement cell shape.

Role of AtTPS6 in Determining Cell Shape

Key components of cell shape are F-actin and MTs, which are important determinants of cell polarity and cell wall remodeling. Accordingly, the three known classes of genes known to participate in cell morphogenesis in plants are (1) cytoskeletal proteins and proteins regulating the cytoskeleton, (2) proteins regulating polarized secretion, and (3) proteins involved

in cell wall synthesis or remodeling. Many mutants in Arabidopsis that are defective in the morphogenesis of both pavement cells and trichomes are affected in either F-actin or MTs. Loss of function of components of the Arp2/3 actin-nucleating complex causes reduced lobe expansion in pavement cells and distorted trichomes that display swollen stalks and retarded branch expansion (Mathur, 2005). Defects in the stability or order of MTs result in distinct phenotypes such as reduced trichome branching and waviness of the jigsaw puzzle-shaped pavement cells by increasing expansion of the sinus region (Fu et al., 2002, 2005; Mathur, 2005). In contrast, increased stability or ordering of MTs results in increased branching of trichomes and inhibition of lobe formation in pavement cells (Fu et al., 2002, 2005; Li et al., 2003; Mathur et al., 2003; Mathur, 2005). Interestingly, from our analysis of both loss-of-function and overexpression phenotypes, we demonstrated that AtTPS6, which possesses both TPS and TPP functions, is involved in the control of pavement cell shape and trichome branching. This is reminiscent of defects in MT organization and future investigations can address this.

Potential interaction between sugar metabolism and actin organization and dynamics is suggested by ARP2/3-defective mutants that have altered responses to sugars (Li et al., 2003). Our findings show that a sugar catabolic enzyme can have an influence on a cytoskeleton-mediated process and suggest an interaction between sugar metabolism and cytoskeletal organization and dynamics.

The obvious question that arises is how AtTPS6 could be involved in the determination of cell shape. One possibility is that trehalose-6-P or a related metabolite could serve as a signal in controlling the MT organization necessary for cell shape determination as has been demonstrated for the morphogenesis of pavement cells (Fu et al., 2002, 2005). Although speculative, it should be possible to test this hypothesis by investigating the effect of trehalose-6-P or *csp-1* and *csp-2* on ROP GTPase signaling during the formation of pavement cell lobes (Fu et al., 2002, 2005). Another possibility is that AtTPS6 could be involved directly in the transcriptional regulation of genes encoding proteins involved in cytoskeletal organization (see below). This possibility is consistent with our observation that the cell shape phenotypes were not reported for *AtTPS1* (Blázquez et al., 1998; van Dijken et al., 2004) or other the class II *AtTPS* genes that we examined. This transcriptional hypothesis is also consistent with our findings that *csp-1* and *csp-2* had pleiotropic effects on developmental processes.

Role of *AtTPS6* in Development

Several previous reports have suggested that trehalose-6-P may be acting as a regulatory molecule involved in metabolism and embryo development (Eastmond et al., 2002). Three different *tps1* T-DNA alleles are embryo lethal, show reduced root growth, and affect the transition to flowering (van Dijken et al., 2004). Interestingly, these phenotypes were not seen with *csp-2*. One explanation may be related to the tissue-specific expression profile of the genes. Whereas *AtTPS6* is expressed ubiquitously, *AtTPS1* is expressed at low levels and concentrated in the flower buds, siliques, and young rosettes (van Dijken et al., 2004). The more ubiquitous expression profile of *AtTPS6* may also explain its broader effects on development and suggest that this gene may play a more central role in modifying development. Conversely, *AtTPS1* may play a more specialized role in modifying embryo or flower development.

The *csp-1* point mutation in the synthase domain of *AtTPS6* results in cell shape, leaf, and branching phenotypes. It also imparts a drought-tolerant phenotype (S.N. Chary and N.V. Raikhel, unpublished data). Although we do not know at this time whether the AtTPS6 protein is present in vivo, the mutant displays detectable gene expression, indicating that the point mutation may be affecting these plant developmental phenotypes within the context of altered protein function. The T-DNA null allele *csp-2* results in the pavement cell shape defect only and not in developmental phenotypes observed in *csp-1*. This indicates that the point mutation in *csp-1* alters a synthase domain function necessary for modulating development (in addition to cell shape). The cell shape phenotype is more mysterious. Although we do not fully understand the basis for the developmental phenotypes in the null and point mutants, one speculation is that the null mutant *csp-2* does not cause developmental defects because there is no phosphatase domain that may be important for the developmental phenotypes. In the point mutant *csp-1*, the interaction of the altered synthase domain, plus an active phosphatase domain, may be necessary for the developmental phenotype. It is also conceivable that the null mutant fails to display developmental defects due to gene redundancy. Overall, this hints at the complex role that AtTPS6 may play in plant development.

There is recent evidence that the maize protein *RAMOSA3* (TPP) affects the development of inflorescence branching via possible interaction with *RAMOSA1* (a predicted transcriptional regulator). However, there is no evidence for interaction between the transcription machinery and AtTPS6. In the case of *csp-1*, the ethyl methanesulfonate mutation confers a recessive phenotype, suggesting a loss of function that results in altered cell shape, decreased trichome branching, slower growth, and altered leaf morphology. This is supported by the null mutant *csp-2*, which displayed the cellular phenotype (but not the developmental phenotypes). Furthermore, the increase in rosette leaf size and trichome branching among overexpression lines suggests that *AtTPS6* acts in a positive manner to affect development. This notion is also supported by the fact that increased expression of AtTPS6 among category I overexpression mutants results in an apparent increase in apical dominance. The observation

that mild overexpression (category II) results in reduced apical dominance similar to that observed in *csp-1* cannot be explained fully at this time. However, it indicates that the processes affected by the mutated gene and mild overexpression are impacting similar developmental pathways.

MATERIALS AND METHODS

Plant Materials and Plant Growth

T-DNA insertion mutant seed was obtained from the Arabidopsis Biological Resource Center. Arabidopsis (*Arabidopsis thaliana*) ecotype Col, *csp-1* mutant (35S:δ-TIP::GFP in Col background), and other mutants were grown on one-half-strength Murashige and Skoog medium containing 1% Suc and 0.8% phytoagar. Plates were placed in a 4°C chamber for 2 d in the dark for vernalization and allowed to germinate and grow at 22°C under long-day conditions (18 h light/6 h dark). After 7 d, seedlings were transplanted to Promix and grown under the same long-day conditions. For the F2 segregating population, seeds were germinated on thin Universal lids (Costar) on one-half-strength Murashige and Skoog medium with 1% Suc and 0.6% phytoagar and grown further at 22°C under long-day conditions in a growth chamber with the seedlings positioned vertically. For all crosses, floral buds of *csp-1* (Col background) were dissected and pollinated using mature pollen from L*er* flowers.

Plant Transformation and Positional Cloning

Arabidopsis ecotype Col plants were transformed with all constructs using *Agrobacterium tumefaciens* GV3101 (pMP90) by the floral-dip method (Clough and Bent, 1998). The *csp-1* mutant was crossed to L*er* ecotype. F1 heterozygotes from this cross were self-fertilized to generate an F2 mapping population. F2 recombinants were screened on an automated BD-Biosciences Pathway confocal microscope.

Expression Array-Based Mapping

Leaf tissue of equal amounts was collected from each of 100 F2 mutant and wild-type plants from a segregating population using a leaf punch and frozen in liquid nitrogen. Tissues were ground to a fine powder and genomic DNA was isolated using DNAzol (Invitrogen). Three hundred nanograms of genomic DNA from each pool were randomly biotin labeled by using the Bioprime DNA labeling system (Invitrogen). The fragmented biotin-labeled DNA (approximately 25–50 bp) was purified using a Qiagen gel purification system and the resulting probe was used for hybridizing to the Arabidopsis genome array ATH1 (24K). Microarray hybridization, staining, washing, and scanning were performed according to the manufacturer (Affymetrix). Scanned cell files were read and analyzed by the freely available statistical package R (http://www.r-project.org; Ihaka and Gentleman, 1996) according to Borevitz et al. (2003).

Fine Mapping

Fine mapping was performed on individual F2 recombinants using simple sequence length polymorphism and BAC markers. PCR reactions were performed and products were resolved on 4% Metaphor agarose gels stained with ethidium bromide. Primers were designed for all genes on BAC T23K23 and genes were PCR amplified by using genomic DNA from the *csp-1* mutant as a template. PCR products were sequenced with overlapping primers every 500 bp. Sequencing, contig assembly, and mutation search were performed with PHRED/PHRAP and CONSED (http://www.phrap.org/phredphrapconsed.html).

Expression Analysis by RT-PCR

Tissues from roots, stems, rosette leaves, cauline leaves, flowers, and siliques of mature Arabidopsis ecotype Col were frozen in liquid nitrogen and ground to fine powder. RNA was isolated using the Qiagen plant RNA preparation kit according to manufacturer. One-step RT-PCR was performed using 0.5 μg of total RNA template using the Platinum quantitative RT-PCR ThermoScript one-step system (Invitrogen). Gene-specific primers of TPS6 were as follows:TPS6 F, 5′-ATGGTTTCAAGATCGTATTCA-3′; and TPS6 R, 5′-GTCCAATGTATCCTCTCTTAG-3′.

As an endogenous standard for relative RT-PCR, 18S ribosomal RNA was amplified using Universal 18S rRNA primers in a 2:8 ratio of 18S rRNA primers to competimers (Ambion). The template RNA for 18S rRNA control reactions consisted of 0.5 μg of total RNA from mouse liver (Ambion). RT was performed at 50°C for 20 min, after which PCR was performed in a total reaction volume of 50 μL using PCR cycling conditions of 95°C, 5 min; 94°C, 15 s; 65°C, 30 s; 72°C, 1 min; and 72°C, 4 min for 32 cycles.

DNA Constructs for Complementation and Overexpression

AtTPS6 was PCR amplified from genomic DNA of Arabidopsis ecotype Col using the following primers: TPS6F, 5′-GCTCGATCCACCTAGGCTTGCCTGTTTCGAGCTATGAG-3′; and TPS6R, 5′-CGTAGCGAGACCACAGGAAACAGGAGTGATCTGGTCTG-3′. The amplified PCR fragment was cloned into the pDONOR207 vector after confirming the sequence; the insert was integrated into the pBIN-GW binary vector and used to transform *csp-1* as described above. T1 seeds were germinated on Murashige and Skoog with 50 μg/mL kanamycin. Kanamycin-resistant seedlings were transplanted into Promix pots and propagated to T2 generation. Selected transgenic lines resistant to kanamycin were grown to the T3 generation to obtain homozygous lines.

The *AtTPS6* coding region was PCR amplified using gene-specific primers from genomic DNA of Arabidopsis ecotype Col. Primers were TPS6-*Bam*HI, 5′-CAGCTGGATCCATGGTTTCAAGATCGTATTCAAATCTG-3′; and TPS6-*Xba*I, 5′-TGTACTCTAGATTAGCCTGTGTAGTAGTTAGATGGAGC-3′. The amplified PCR fragment was digested with appropriate restriction enzymes and purified and cloned into the modified plant binary vector pZP111 containing a 35S promoter with a translational enhancer (Ω-leader sequence). The construct was transformed and independent kanamycin-resistant lines were isolated.

Yeast Expression Constructs

The coding region of *AtTPS6* was PCR amplified from Arabidopsis genomic DNA using a primer with 5′ *Kpn*I and 3′ *Xho*I restriction sites for compatible restriction sites for cloning into the yeast (*Saccharomyces cerevisiae*) expression vector pYES2. The primers were: TPS6-*Kpn*I, 5′-GGGGGTACCATGGTTTCAAGATCGTATTCAAATCTG-3′; and TPS6-*Xho*I, 5′-GGGCTCGATTAGCCTGTGTAGTAGTTAGATGGAGC-3′.

PCR-amplified products were digested with *Kpn*I and *Xho*I and ligated to *Kpn*I-*Xho*I-digested pYES2.

The *AtTPS6* construct in pYES2 was used to transform the yeast *tps1* and *tps2* deletion mutants (Operon Biosystems).

Confocal Microscopy

Ten-day-old seedlings of the parental line, mutants, and overexpression lines were examined on a Leica SP2 confocal microscope, using 20×/0.7NA and 63×/1.2NA HC PL Apo water objectives. The 488-nm argon laser line was used for excitation of GFP and emission was collected between 500 and 600 nm. FM4-64 was excited at 488 nm and detected between 600 and 750 nm. For mapping, the BD Biosciences Pathway HT imaging system was used with a UAPO/340 20×/0.75NA dry objective and custom filter wheels containing the Semrock Brightline GFP-3035B filter set with 472/30-nm excitation and 520/35-nm emission.

Scanning Electron Microscopy

Parental and mutant leaves were flash frozen by immersion in 1,1-difluoroethane in a liquid nitrogen-cooled mortar, then immediately transferred to the scanning electron microscope vacuum chamber for scanning at 15 keV using back-scattered electron detection on a Hitachi TM-1000 tabletop scanning electron microscope.

Morphometric Analysis

Trichome branch lengths were measured from scanning electron micrographs using Imaging Research MCID Elite software. The lengths and widths

of parental and *csp-1* mutant hypocotyl cells were tabulated from cells using 20× Leica confocal micrographs. For the parental line, 168 cells were examined and for the *csp-1* mutant 209 cells were examined from independent seedlings.

Sequence data from this article can be found in the GenBank/EMBL data libraries under accession numbers At1g68020 (*AtTPS6*), *csp-2* (SALK T-DNA insertion mutant SALK_150965.55.25.x).

Supplemental Data

The following materials are available in the online version of this article.

Supplemental Figure S1. Mapping of the *csp-1* locus using expression array bulk segregant analysis.

Supplemental Figure S2. Multiple alignments of AtTPS family members in Arabidopsis.

Supplemental Figure S3. Class I and class II TPSs in Arabidopsis are distinct.

ACKNOWLEDGMENTS

We thank Justin Borevitz for his discussions on expression array mapping analysis. We are also very grateful to Dr. Maarten Chrispeels and Dr. Zhenbiao Yang for many helpful suggestions and critical reading of the manuscript.

Received August 15, 2007; accepted October 19, 2007; published November 2, 2007.

LITERATURE CITED

Adams RP, Kendall E, Kartha KK (1990) Comparison of free sugars in growing and desiccated plants of *Selaginella lepidophylla*. Biochem Syst Ecol **18:** 107–110

Alonso JM, Stepanova AN, Leisse TJ, Kim CJ, Chen H, Shinn P, Stevenson DK, Zimmerman J, Barajas P, Cheuk R, et al (2003) Genome-wide insertional mutagenesis of *Arabidopsis thaliana*. Science **301:** 653–657

Augier J (1954) The biochemistry of the North American algae, *Tuomeya-fluviatillis*. Compt Rend **239:** 87–89

Avila EL, Zouhar J, Agee AE, Carter DG, Chary SN, Raikhel NV (2003) Tools to study plant organelle biogenesis point mutation lines with disrupted vacuoles and high-speed confocal screening of green fluorescent protein-tagged organelles. Plant Physiol **133:** 1673–1676

Bell CJ, Ecker JR (1994) Assignment of 30 micro satellite loci to the linkage map of *Arabidopsis*. Genomics **9:** 137–144

Blázquez MA, Lagunas R, Gancedo C, Gancedo JM (1993) Trehalose-6-phosphate, a new regulator of yeast glycolysis that inhibits hexokinases. FEBS Lett **329:** 51–54

Blázquez MA, Santos E, Flores CL, Martínez-Zapater JM, Salinas J, Gancedo C (1998) Isolation and molecular characterization of the *Arabidopsis TPS1* gene, encoding trehalose-6-phosphate synthase. Plant J **13:** 685–689

Bonini BM, vanVaeck C, Larsson C, Gustafsson L, Ma P, Winderickx J, van Dijck P, Thevelein JM (2000) Expression of *Escherichia coli OTSA* in a *Saccharomyces cerevisiae tps1* mutant restores trehalose-6-P levels and partially restores growth and fermentation with glucose and control of glucose influx into glycolysis. Biochem J **350:** 261–268

Borevitz JO, Liang D, Plouffe D, Chang HS, Zhu T, Weigel D, Berry CC, Winzeler E, Chory J (2003) Large-scale identification of single-feature polymorphisms in complex genomes. Genome Res **13:** 513–523

Clough SJ, Bent AF (1998) Floral dip: a simplified method for *Agrobacterium*-mediated transformation of *Arabidopsis thaliana*. Plant J **16:** 735–743

Crowe JH, Hoekstra FA, Crowe LM (1992) Anhydrobiosis. Annu Rev Physiol **54:** 579–599

Cutler SR, Ehrhardt DW, Griffitts JS, Somerville CR (2000) Random GFP:cDNA fusions enable visualization of subcellular structures in cells of Arabidopsis at a high frequency. Proc Natl Acad Sci USA **97:** 3718–3723

Deeks MJ, Hussey PJ (2003) Arp2/3 and the shape of things to come. Curr Opin Plant Biol **6:** 561–567

De Virgilio C, Burckert N, Bell W, Jeno P, Boller T, Wiemken A (1993) Disruption of *TPS2*, the gene encoding the 100-kDa subunit of the trehalose-6-phosphate synthase/phosphatase complex in *Saccharomyces cerevisiae*, causes accumulation of trehalose-6-phosphate and loss of trehalose-6-phosphate phosphatase activity. Eur J Biochem **212:** 315–323

Eastmond PJ, van Dijken AJ, Spielman M, Kerr A, Tissier AF, Dickinson HG, Jones JD, Smeekens SC, Graham IA (2002) Trehalose-6-phosphate synthase 1, which catalyses the first step in trehalose synthesis, is essential for Arabidopsis embryo maturation. Plant J **29:** 225–235

Elbein AD (1974) The metabolism of α,α-trehalose. Adv Carbohydr Chem Biochem **30:** 227–256

Elbein AD, Pan YT, Pastuszak I, Caroll D (2003) New insights on trehalose: a multifunctional molecule. Glycobiology **13:** 17R–27R

Fillinger S, Chaveroche MK, van Dijck P, de Vries R, Ruijter G, Thevelein J, d'Enfert C (2001) Trehalose is required for the acquisition of tolerance to a variety of stresses in the filamentous fungus *Aspergillus nidulans*. Microbiology **147:** 1851–1862

Frank M, Smith L (2002) A small, novel protein highly conserved in plants and animals promotes the polarized growth and division of maize leaf epidermal cells. Curr Biol **12:** 849–853

Fu Y, Gu Y, Zheng Z, Wasteneys G, Yang Z (2005) *Arabidopsis* interdigitating cell growth requires two antagonistic pathways with opposing action on cell morphogenesis. Cell **120:** 676–700

Fu Y, Li H, Yang Z (2002) The ROP2 GTPase controls the formation of cortical fine F-actin and the early phase of directional cell expansion during *Arabidopsis* organogenesis. Plant Cell **14:** 777–794

Goddijn O, Smeekens S (1998) Sensing trehalose biosynthesis in plants. Plant J **14:** 143–146

Goddijn OJ, van Dun K (1999) Trehalose metabolism in plants. Trends Plant Sci **4:** 315–319

Gómez LD, Baud S, Gilday A, Li Y, Graham IA (2006) Delayed embryo development in the *ARABIDOPSIS TREHALOSE-6-PHOSPHATE SYNTHASE 1* mutant is associated with altered cell wall structure, decreased cell division and starch accumulation. Plant J **46:** 69–84

Gómez LD, Baud S, Graham IA (2005) The role of trehalose-6-phosphate synthase in *Arabidopsis* embryo development. Biochem Soc Trans **33:** 280–282

Ihaka R, Gentleman R (1996) R: a language for data analysis and graphics. J Comput Graph Statist **5:** 299–314

Jang IC, Oh SJ, Seo JS, Choi WB, Song SI, Kim CH, Kim YS, Seo HS, Choi YD, Nahm BH (2003) Expression of a bifunctional fusion of the *Escherichia coli* genes for trehalose-6-phosphate synthase and trehalose-6-phosphate phosphatase in transgenic rice plants increases trehalose accumulation and abiotic stress tolerance without stunting growth. Plant Physiol **131:** 516–524

Karim S, Aronsson H, Ericson H, Pirhonen M, Leyman B, Welin B, Mantyla E, Palva ET, Van Dijck P, Holmstrom KO (2008) Improved drought tolerance without undesired side effects in transgenic plants producing trehalose. Plant Mol Biol (in press)

Leyman B, van Dijck P, Thevelein JM (2001) An unexpected plethora of trehalose biosynthesis genes in *Arabidopsis thaliana*. Trends Plant Sci **6:** 510–513

Li S, Blanchoin L, Yang Z, Lord EM (2003) The putative Arabidopsis Arp2/3 complex controls leaf cell morphogenesis. Plant Physiol **132:** 2034–2044

Mathur J (2004) Cell shape development in plants. Trends Plant Sci **12:** 583–590

Mathur J (2005) The ARP2/3 complex: giving plant cells a leading edge. Bioessays **27:** 377–387

Mathur J, Mathur N, Kernebeck B, Hulskamp M (2003) Mutations in actin-related proteins 2 and 3 affect cell shape development in *Arabidopsis thaliana*. Plant Cell **15:** 1632–1645

Müller J, Boller T, Wiemken A (1995) Trehalose and trehalase in plants: recent developments. Plant Sci **112:** 1–9

Newman Y, Ring SG, Colaco C (1993) The role of trehalose and other carbohydrates in biopreservation. Biotechnol Genet Eng Rev **11:** 263–294

Oppenheimer DG (1998) Genetics of plant cell shape. Curr Opin Plant Biol **1:** 520–524

Paul M, Pellny T, Goddijn O (2001) Enhancing photosynthesis with sugar signals. Trends Plant Sci **6:** 197–200

Pellny TK, Ghannoum O, Conroy JP, Schluepmann H, Smeekens S, Andralojc J, Krause KP, Goddijn O, Paul MJ (2004) Genetic modification

of photosynthesis with *E. coli* genes for trehalose synthesis. Plant Biotechnol J **2:** 71–82

Pilon-Smits EAH, Terry N, Sears T, Kim H, Zayed A, Hwang S, van Dun K, Voogd E, Verwoerd TC, Krutwagen RWHH, et al (1998) Trehalose producing transgenic tobacco plants show improved growth performance under drought stress. J Plant Physiol **152:** 525–532

Qiu JL, Jilk R, Marks MD, Szymanski DB (2002) The *Arabidopsis SPIKE1* gene is required for normal cell shape control and tissue development. Plant Cell **14:** 101–118

Romero C, Belles JM, Vaya JL, Serrano R, Culianez-Macia FA (1997) Expression of the yeast trehalose-6-phosphate synthase gene in transgenic tobacco plants: pleiotropic phenotypes include drought tolerance. Planta **201:** 293–297

Satoh-Nagasawa NS, Nagasawa N, Malcomber S, Sakai H, Jackson D (2006) A trehalose metabolic enzyme controls inflorescence architecture in maize. Nature **441:** 227–230

Schellmann S, Hulskamp M (2005) Epidermal differentiation: trichomes in Arabidopsis as a model system. Int J Dev Biol **49:** 579–584

Schluepmann H, Pellny T, van Dijken A, Smeekens S, Paul M (2003) Trehalose 6-phosphate is indispensable for carbohydrate utilization and growth in *Arabidopsis thaliana.* Proc Natl Acad Sci USA **100:** 6849–6854

Smith LG (2003) Cytoskeletal control of plant cell shape: getting the fine points. Curr Opin Plant Biol **6:** 63–73

Smith LG, Hake S, Sylvester AW (1996) The tangled-1 mutation alters cell division orientations throughout maize leaf development without altering leaf shape. Development **122:** 481–489

Smith LG, Oppenheimer DG (2005) Spatial control of cell expansion by the plant cytoskeleton. Annu Rev Cell Dev Biol **21:** 271–295

van Dijken AJH, Schluepmann H, Smeekens SCM (2004) Arabidopsis trehalose-6-phosphate synthase 1 is essential for normal vegetative growth and transition to flowering. Plant Physiol **135:** 969–977

Van AL, Hofmann S, Bulaya B, de Koning W, Sierkstra L, Neves MJ, Luyten K, Alijo R, Ramos J, Coccetti P (1993) Molecular cloning of a gene involved in glucose sensing in the yeast *Saccharomyces cerevisiae.* Mol Microbiol **8:** 927–943

van Vaeck C, Wera S, Van Dijck P, Thevelein JM (2001) Analysis and modification of trehalose 6-phosphate levels in the yeast *Saccharomyces cerevisiae* with the use of *Bacillus subtilis* phosphotrehalase. Biochem J **353:** 157–162

Vogel G, Fiehn O, Jean-Richard-dit-Bressel L, Boller T, Wiemken A, Aeschbacher RA, Wingler A (2001) Trehalose metabolism in *Arabidopsis*: occurrence of trehalose and molecular cloning and characterization of trehalose-6-phosphate synthase homologues. J Exp Bot **52:** 1817–1826

Wasteneys GO, Galway ME (2003) Remodeling the cytoskeleton for growth and form: an overview with some new views. Annu Rev Plant Biol **54:** 691–722

Wiemken A (1990) Trehalose in yeast, stress protectant rather than reserve carbohydrate. Antonie Van Leeuwenhoek **58:** 209–217